Cationic nanoliposomes are efficiently taken up by alveolar macrophages but little access dendritic cells and interstitial macrophages in the normal and CpG-stimulated lungs

Rita Vanbever[a*], Cristina Loira-Pastoriza[a], Nicolas Dauguet[b], Caroline Hérin[a], Saloua Ibouraadaten[c], Kevin Vanvarenberg[a], Bernard Ucakar[a], Donatienne Tyteca[d], François Huaux[c]

[a]Louvain Drug Research Institute, Advanced Drug Delivery & Biomaterials, Université catholique de Louvain (UCLouvain), Brussels, Belgium
[b]de Duve Institute, Flow Cytometry and Cell Sorting platform, UCLouvain, Brussels, Belgium
[c]Institut de Recherche Expérimentale et Clinique, Louvain centre for Toxicology and Applied Pharmacology, UCLouvain, Brussels, Belgium.
[d]de Duve Institute, Cell Biology, UCLouvain, Brussels, Belgium

*Corresponding author: Advanced Drug Delivery & Biomaterials, Louvain Drug Research Institute, Université catholique de Louvain, Avenue E. Mounier, 73 boite B1.73.12, 1200 Brussels, Belgium. Tel: +32 2 764 73 25. Fax: +32 2 764 73 98. E-mail address: rita.vanbever@uclouvain.be

Abstract:

The purpose of this study was to assess whether cationic nanoliposomes could address tumor vaccines to dendritic cells in the lungs *in vivo*. Nanoliposomes were prepared using a cationic lipid, dimethylaminoethanecarbamoyl-cholesterol (DC-cholesterol) or dioleoyltrimethylammoniumpropane (DOTAP), and dipalmitoylphosphatidylcholine (DPPC), the most abundant phospholipid in lung surfactant. The liposomes presented a size below 175 nm and they effectively entrapped tumor antigens, an oligodeoxynucletotide containing CpG motifs (CpG) and the fluorescent dye calcein used as a tracer. Although the liposomes could permanently entrap a large fraction of the actives, they could not sustain their release *in vitro*. Liposomes made of DOTAP were safe to respiratory cells *in vitro* while liposomes composed of DC-cholesterol were cytotoxic. DOTAP nanoliposomes were mainly taken up by alveolar macrophages following delivery to the lungs in mice. Few dendritic cells took up the liposomes and interstitial macrophages did not take up liposomal calcein more than they took up soluble calcein. Stimulation of the innate immune system using liposomal CpG strongly enhanced uptake of calcein liposomes by all phagocytes in the lungs. Although a small percentage of dendritic cells took up the nanoliposomes, alveolar macrophages represented a major barrier to dendritic cells access in the lungs.

Keywords: nanoliposomes, lungs, macrophages, dendritic cells.

Abbreviations:

AMs, alveolar macrophages; APCs, antigen-presenting cells; BAL, bronchoalveolar lavage; BSA, bovine serum albumin; CpG, unmethylated oligodeoxynucleotides containing CpG motifs; DCs, dendritic cells; DC-cholesterol, 3β-[N-(N',N'-dimethylaminoethane)-carbamoyl]cholesterol; DOPE, 1,2-dioleoyl-sn-glycero-3-phosphoethanolamine; DOTAP, 1,2-dioleoyl-3-trimethylammonium-propane; DPPC, 1,2-dipalmitoylphosphatidylcholine; λ, wavelength; EE, encapsulation efficiency; FBS, fetal bovine serum; HBSS, Hank's Balanced salt solution; HPLC, high-performance liquid chromatography; IMs, interstitial macrophages; IL-6, interleukin-6; MEM, minimum essential medium; MFIs, median fluorescence intensities; MHC-II, major histocompatibility complex II; MTS, (3-(4,5-dimethylthiazol-2-yl)-5-(3-carboxymethoxyphenyl)-2-(4-sulfophenyl)- 2H-tetrazolium); MTT, 3-(4,5-dimethylthiazol-2-yl)-2,5-diphenyltetrazolium bromide; PBS, phosphate buffer saline; PDI, polydispersity index; SD, standard deviation; TFA, trifluoroacetic acid; TLR9, toll-like receptor 9.

Introduction

Lung cancer is the leading cause of cancer-related deaths worldwide, accounting for 1.7 million deaths in 2015[1]. Immunotherapy brings new hope to the fight against lung cancer. Immunotherapy stimulates the host immune system to recognize tumor cells as non-self and eliminate them. Immune checkpoint inhibitors have been the first immunotherapy approved in lung cancer. Immune checkpoint blockade can enhance T cell activation and effector functions resulting in a swift tissue inflammatory response. In addition, several therapeutic vaccines against tumor associated antigens have been developed and tested in large clinical trials[2]. However, experience in the clinic has been disappointing with a durable benefit in only limited subgroups of patients with lung cancer and with modest survival extensions. Nevertheless, personalized neoantigen vaccines have revived this immunotherapy approach and have recently shown promising results. Melanoma patients treated with up to twenty predicted personal tumor neoantigens have either shown no cancer recurrence after two years or, recurrence and complete tumour regression after checkpoint blockade[3]. Therefore, highly heterogenous tumours can be targeted with a personal multi-peptide neoantigen vaccine.

Immune modulation in the lungs may represent a direct approach to treat respiratory disorders such as lung cancer. Delivery of vaccines locally in the lungs has been widely investigated for an improved protection against respiratory pathogens[4]. In fact, dendritic cells (DCs) and macrophages are strategically located for antigen capture and presentation and local immunization generates immunity at the natural site of infection. However, the potential of pulmonary vaccination to treat lung cancer has never been investigated.

Dendritic cells and macrophages are the major phagocyte population that can function as professional antigen-presenting cells (APCs) in the lungs[5]. Among these, DCs are specialized in antigen uptake and processing and translocate quickly to draining lymph nodes to present antigen to naive T cells and help naive T cells to differentiate into effector T cells. Dendritic

cells are found in the lung parenchyma and beneath the epithelium in the airways. Dendritic cells extend dendrites through the epithelial layer into the airway lumen to sample antigen[5]. Alveolar macrophages (AMs) are located in the airway and alveolar lumen while interstitial macrophages (IMs) are situated inside the lung interstitium. Interstitial macrophages express the major histocompatibility complex II (MHC-II) which displays exogenous peptide fragments on the cell surface for T cells recognition[5]. Alveolar macrophages are poor at presenting antigens to T cells and they dampen immune responses to inhaled antigens[6]. Alveolar macrophages are equipped with a set of inhibitory surface receptors that prevent their unrestrained activation and guarantee a low inflammatory environment in the lungs. However, AMs can also respond in a pro-inflammatory manner to a more pathogenic stimulus. The initiation of inflammation requires a combination of events that override the inhibitory mechanisms that regulate AMs[6].

Because DCs control a substantial part of the adaptive immune response, targeting DCs with an antigen-delivery system provides potential to develop potent vaccines. Particulate delivery systems offer a natural targeting to APCs as a result of particle phagocytosis. In addition, particle carriers can co-encapsulate and co-deliver adjuvants and antigens to APCs and protect the actives from degradation *in vivo*[7]. The uptake of particle carriers by lung phagocytes is determined by their particle size, surface-charge and shape. Alveolar macrophages clear nanoparticles less efficiently than they clear microparticles[8]. Blank et al showed that polystyrene particles with sizes ranging from 20 nm to 1,000 nm were mainly taken up by AMs following intranasal instillation in mice but that DCs also took up the particles and especially the smallest ones[9]. Fromen et al demonstrated that cationic hydrogel nanoparticles were preferentially taken up by lung DCs while anionic nanoparticle counterparts were more readily internalized by AMs[10]. The larger DC uptake of cationic nanoparticles was associated with an increased expression of the chemo-attractants Ccl2 and Cxc10. Yet, no study has investigated whether immune stimulation of the lung tissue alters the fate of nanoparticles.

The goal of this research was to assess whether cationic nanoliposomes could address tumor vaccines to DCs in the lungs. Liposomes can be prepared with lipids endogenous to the lungs and show excellent safety. As a result, liposomes are currently the only carrier for pulmonary delivery that has reached clinical development[11]. In addition, cationic lipids present immunostimulatory properties[12]. We prepared cationic nanoliposomes co-encapsulating tumor antigens and an oligodeoxynucleotide containing unmethylated cytosine-phosphate-guanine motifs (CpG) as a vaccine adjuvant. Liposomes were produced by the film hydration method using two cationic lipids, DC-cholesterol and DOTAP, largely used to encapsulate anionic nucleic acids, together with DPPC, the main phospholipid in lung surfactant[13]. We characterized the particle size, surface charge, release properties and cytotoxicity of the nanoliposomes and we investigated their uptake by lung phagocytes *in vitro* and *in vivo*. The fate of the nanoliposomes was investigated *in vivo* in unstimulated lungs as well as in lungs stimulated with CpG in order to assess whether immune stimulation could affect nanoliposomes uptake.

Experimental Section

Preparation of liposomes

Liposomes were prepared by the film hydration method using 3β-[N-(N',N'-dimethylaminoethane)-carbamoyl]cholesterol (DC-cholesterol; Avanti Polar Lipids; AL, USA), 1,2-dipalmitoylphosphatidylcholine (DPPC; Lipoid GMBH; Ludwigshafen, Germany) and 1,2-dioleoyl-3-trimethylammonium-propane (DOTAP; Avanti Polar Lipids; Alabaster, AL, USA). DC-cholesterol (5.2 mg) and DPPC (4.8 mg) or DOTAP (5.9 mg) and DPPC (4.1 mg) were dissolved in chloroform (750 µl; analytical grade; VWR International, Leuven, Belgium). These lipid quantities corresponded to a cationic lipid:DPPC molar ratio of 3:2. A lipid film was prepared by rotary evaporation of the lipids solution under vacuum. 200 µg of antigens (Melan $A_{(26-35)}$ and $Gp100_{(209-217)}$; Proteogenix, Schiltigheim, France) and/or 200 µg of phosphorothioate linked CpG oligonucleotide (5'TCGTCGAACGTTCGAGATGAT 3'; CpG; Eurogentec; Seraing, Belgium) or 150 µg of calcein (high purity; ThermoFischer Scientific, Aalst, Belgium) in 1 ml of water were added to the film. Five cycles of freezing and thawing were conducted in order to prepare multilamellar vesicles. Liposomes were downsized by extrusion through polycarbonate membranes of 200 nm pore size (Whatman; Diegem, Belgium) using a mini-extruder (Avanti Polar Lipids). They were then concentrated by ultrafiltration (Vivaspin 2, 100 000 molecular weight cut-off; Sartorius, Stonehouse, Gloucestershire, UK) at 3000 g and 4°C for 1h. The liposomes were prepared the same day as *in vitro* or *in vivo* experiments.

Physical characterization of the liposomes

Liposome size, polydispersity index (PDI) and zeta potential were measured with a Nanosizer ZS (Malvern, UK). Liposome stability at room temperature was assessed by measuring liposome size, zeta potential and leakage of the Gp100 peptide, CpG and calcein from the liposomes over two weeks.

Liposome morphology and the number of lipid bilayers were observed by transmission electron microscopy (Philips Electron Microscope CM12/STEM)**.** Liposome suspension was diluted 500-times in ultrapure water. A negative staining was made by mixing liposome dispersion with a 4% tungstophosphoric acid (Merck, Darmstadt, Germany) in a 1:1 (v/v) ratio. Stained liposomes were deposited on copper grids (Formvar 300 Mesh Cu grids, Agar Scientific, Essex, UK). The excess liquid was removed and grids were allowed to dry in a Petri box. Microscopic analyses were carried out at a magnification of 60,000.

The amount of the different compounds encapsulated in liposomes was measured indirectly on liposome filtrates. The peptide antigens were assayed by high-performance liquid chromatography (HPLC; Agilent 1100 series, Agilent Technologies, Palo Alto, CA). Solvent A was composed of ultrapure water and 0.1% trifluoroacetic acid (TFA; Carl Roth GmbH + Co. KG; Karlsruhe, Germany), and solvent B was composed of acetonitrile (analytical grade) and 0.1% TFA. A linear gradient of Solvent A (80 to 50 %) in 15 minutes was used. Fifty microliters of sample filtrate or standard were injected to a reverse phase column (Nucleodur C18, 150 mm, 4µm, Macherey Nagel, Düren, Germany) at room temperature and detection was performed at a wavelength of 220 nm. The CpG was quantified by the oligreen assay (ThermoFischer Scientific). The filtrate was mixed with the oligreen® reagent at 1:1 (v/v) ratio

and fluorescence was measured ($\lambda_{excitation}$: 485 nm; $\lambda_{emission}$: 520 nm) with a Victor 2 luminometer (Perkin Elmer). The amount of calcein in filtrates was measured through its fluorescence ($\lambda_{excitation}$: 494 nm; $\lambda_{emission}$: 518 nm). The leakage of the different compounds from the liposomes was assessed following storage at room temperature for 0, 7 or 14 days by measuring compound concentration in the liposome suspension medium after removal of the liposomes by ultrafiltration.

To evaluate the progressive release of peptides, CpG or calcein from the liposomes, concentrated liposomes were poured into a dialysis bag (Spectra Por 1, 6-8 kDa molecular weight cut-off, Spectrum labs, Netherlands). The dialysis bag was kept in phosphate buffer saline (PBS) at 37°C under stirring. Samples were withdrawn at determined times and analyzed by using HPLC, the oligreen reagent or fluorimetry.

Cytotoxicity of the liposomes

The Calu-3 bronchial epithelial cells (ATCC-HBT-55; LGC Standards s.a.r.l; Molsheim, France) were cultured in minimum essential medium (MEM; Life Technologies; Gent, Belgium) containing 10% fetal bovine serum (FBS; Gibco, Merelbeke, Belgium) and maintained at 37°C in 5% CO_2 atmosphere. Murine immature dendritic cells (JAWS II; ATCC-CRL-11904) were cultivated in αMEM containing ribonucleosides, supplemented with 20% FBS, 4 mM L-Glutamine, 5 ng/ml granulocyte-macrophage colony-stimulating factor (PreproTech, UK).

The thiazolyl blue tetrazolium bromide (MTT) test or the CellTiter 96® aqueous one solution cell proliferation assay (MTS) was performed in order to evaluate the cytotoxicity of the liposomes. The MTT test was performed for the adherent Calu-3 cells and the MTS test was for the partially-adherent JAWS II cells. Cells ($1.5x10^4$ cells/well) were seeded in a 96 well plate and allowed to attach overnight. Different concentrations of liposomes (6.2 to 500 µg lipids/ml) were added to the cells and incubated for 24 h. Culture medium and triton 1% were used as negative and positive controls, respectively. After incubation, supernatants were removed and the MTT reagent (Sigma Aldrich; Diegem, Belgium) was added to Calu-3 cells. The MTS reagent (Promega; Leiden; Netherlands) was directly added to JAWS II cells without removing the medium. Incubation was pursued for 3 hours. In case of MTS, absorbance was measured at 490 nm directly after incubation. In case of MTT, dimethyl sulfoxide was used to lyse the cells and to dissolve the formazan crystals. Absorbance was then measured at 560 nm.

Uptake of the liposomes by phagocytes in vitro

Murine MHS alveolar macrophages (ATCC-CRL-2019) were cultured in RPMI 1640 medium (Life Technologies) containing 10% FBS and 0.05 mM 2-mercaptoethanol. Murine J774 macrophages (ATCC-TIB-67) were cultured in Dulbecco's Modified Eagle Medium GlutaMAX (Life Technologies) containing 10% FBS and 100 units/ml penicillin, 100 µg/ml streptomycin (Life Technologies).

5×10^4 MHS, JAWS II or J774 cells/well were seeded in 24 well plates and incubated for 24 hours. The next day, plates were centrifuged (250 g/10 min/4°C) and supernatant was removed. Calcein (5 µg/well) encapsulated in DOTAP liposomes (370 µg lipids/well) or in

solution was added to the wells and incubated at 37°C for 4 h. Non-treated cells were used as control. After incubation, cells were washed 5 times with PBS-bovine serum albumin (BSA) 1%, trypsinized and then resuspended in 300µl PBS before flow cytometric analysis with the FACSVerse Flow Cytometer (BD Biosciences; San Jose; CA; USA). Data were analyzed through FlowJo software (BD Biosciences).

Stimulation of alveolar macrophages by liposomes in vitro

5 x 10^5 MHS cells/well were seeded in 24 well plates and incubated for 24 hours. The next day, plates were centrifuged (250 g/10 min/4°C) and supernatants were removed. Fresh medium and empty DOTAP liposomes (50 µg lipids/well) or CpG in solution (1 µg CpG/well) or in liposomes (1 µg CpG/well in 50 µg lipids/well) were added to the wells and the cells were incubated at 37°C for 2 h. Non-treated cells were used as controls. After the incubation, plates were centrifuged (250 g/10 min/4°C), supernatants were removed and replaced by fresh RPMI medium and the cells were incubated further for 24 h. After a last centrifugation (250 g/10 min/4°C), supernatants were removed and kept at 4°C until assayed for interleukin-6 content by ELISA (Mouse IL-6 DuoSet ELISA; Bio-Techne LTD, Abingdon, UK).

Confocal imaging of the lungs

Animal experiments were approved by the Institutional Animal Care and Use Committee of the Université catholique de Louvain (Permit number: 2012/UCL/MD/006). Female NMRI mice (6 to 9 week-old; Elevage Janvier, Le Genest-St-Isle, France) were anaesthetized by ketamine/xylazine (90/10 mg/kg) intraperitoneal injection. Calcein encapsulated in DOTAP liposomes or in solution was then administered intratracheally to the lungs of the mice at a dose of 5 µg. For intratracheal instillation, mice were placed on their back with a tilt angle of 45˚. A laryngoscope (Penn-Century Inc., Philadelphia, USA) was used to correctly place the bended and blunt needle of a 100 µl precision micro-syringe (Hamilton, Bonaduz, Switzerland) into the trachea. Twenty-five microliters of the calcein solution or calcein liposomes suspension were delivered followed by a 200 µl air bolus using 1 ml syringe having an angled 18 gauge needle with a blunt tip. One hour following administration, the mice were reanesthetized and an abdominal incision was made. The posterior vena cava was cannulated with a Insyte-W™ catheter (Becton Dickinson Infusion Therapy Systems, Sandy, UT, USA) connected via a Connecta (Becton Dickinson Infusion Therapy Systems, Sandy, UT, USA) to two reservoirs containing: (i) 0.9 % (w/v) NaCl and (ii) a fixative solution 4 % (v/v) formaldehyde in 0.9 % (w/v) NaCl[14]. Both the carotid arteries and jugular veins were cut, and solution (i) was perfused via the vasculature at a flow rate of 2 ml/min during 10 min. Then, lung fixation through the pulmonary vasculature was carried out using solution (ii) at a flow rate of 1 ml/min for 10 min. Subsequently, the thoracic cavity was opened and the lungs were removed. Slices of approximately 2 mm of lung lobes were immersed in Draq5™ (Abcam, Cambridge, UK), diluted 1:100 (50 nM) in solution (ii) for 2 min[15]. Then, the slices were briefly immersed in PBS and finally placed into a receptacle (Lab-Tek II chambered coverglass W/cover #1.5 borosilicate sterile; Lab-Tek® Brand products, Rochestern NY, USA) for analysis by confocal laser scanning microscopy. The experiment was repeated twice. Preparations were examined with a LSM 510 microscope (Zeiss, Jena, Germany) using a Plan-Apochromat 20x/0.8

objective (Zeiss, Jena, Germany). Fluorescent emissions from calcein and DRAQ5 were sequentially recorded in the green and far-red channels, respectively. To evaluate the autofluorescence properties of the pulmonary tissue, samples were analyzed with confocal laser scanning microscopy without calcein. The autofluorescence in the green channel was very low considering the intensity of the illuminating laser used.

Flow cytometry

Flow cytometry was used to assess the uptake of calcein liposomes by DCs, AMs and IMs in the murine lungs. Each group of mice comprised 5 animals. Briefly, 1 h after intratracheal instillation of 5 µg calcein in solution or encapsulated in DOTAP liposomes (370 µg lipids), mice were sacrificed by cervical dislocation. Bronchoalveolar lavage (BAL) was performed by cannulating the trachea and flushing the lung lobes with 1 ml of sterile 0.9% saline solution. The obtained lavage fluid was then centrifuged (4°C, 1250 rpm, 10 min) and the cell pellets were used for cellular analysis. The lavaged lungs were infused through the cannula with 1 ml of Hanks' balanced salt solution (Invitrogen, Merelbeke, Belgium) containing 2 mg of Pronase (Sigma-Aldrich, St Louis, MO, USA) to dissociate the lung tissue, and 0.1 mg of DNase (Worthington Biochemical, Lakewood, NJ, USA) to prevent cell aggregation with 1% antibiotic antimycotic and fungizone (25mg/ml; Life Technologies). After 20 minutes at room temperature, lung tissues were removed and mechanically dispersed with a 20 ml syringe. The resulting cell suspension was filtered through a 70 µm filter (BD Biosciences, Bedford, MA, USA).

Pulmonary macrophages and DCs were identified in BAL and lung cell suspensions by using flow cytometry and conventional cell markers[16-18]. Alveolar macrophages ($CD45^{hi}$ $F4/80^{hi}$ $CD64^{hi}$ $CD11c^{hi}$ Siglec-F^{hi} $CD11b^{lo}$ cells), interstitial macrophages ($CD45^{hi}$ $F4/80^{hi}$ $CD64^{hi}$ $CD11c^{hi}$ $CD11b^{hi}$ Siglec-F^{lo} cells) and dendritic cells ($CD45^{hi}$ $CD11c^{hi}$ $MHCII^{hi}$ $F4/80^{lo}$ $CD64^{lo}$ cells) were discriminated following the gating strategy illustrated in Fig. S1. The identification of these three lung sub-populations was performed by using the following fluorochrome-conjugated monoclonal antibodies specific to the mouse antigens: anti-CD45 (clone 30-F11, APC-Cy7; BD Biosciences, Oxford, UK), -F4/80 (clone BM8, APC; eBioscience, Vienna, Austria), -CD11c (clone HL3, PE-Cy7; BD Biosciences), -CD64 (clone X54-5/7.1, PE; BD Biosciences), and -Siglec-F (clone E50-2440, BV421, BD Biosciences) -CD11b (clone M1/70, BV421, BD Biosciences) and -MHCII/I-A/I-E (clone M5/114.15.2, PE; BD Biosciences). Samples were fixed in 1.25% paraformaldehyde in PBS, acquired on a BD LSR Fortessa (BD Biosciences) and analyzed using the FlowJo (TreeStar) software. Median Fluorescence Intensities are not comparable between the two separate experiments presented in Figs 7 and 8 because the PMT voltage used for the detection of calcein-positive cells was different.

The innate immune system in the lungs was stimulated using liposomal CpG in order to see whether stimulation could alter phagocytes uptake of calcein liposomes. Liposome-encapsulated CpG (1 µg of CpG in 50 µg lipids) suspended in 25 µl of PBS was intratracheally instilled in the lungs of mice thrice 5 days apart. Calcein liposomes (5 µg calcein in 370 µg lipids) or solution (5 µg calcein) were then delivered by intratracheal instillation one day after the last administration of CpG liposomes.

Statistical analysis

All results are presented as mean values ± standard deviation (SD). The Kruskal-Wallis and Mann-Whitney tests were used for the statistical analysis of the data in Table 1. Two-way ANOVA test with Bonferroni post-test was used for the statistical analysis of the data in Fig. 2. One-way ANOVA with Dunnet orTukey post-test was used for the statistical analysis of the data in Figs. 3-5. A two-tailed unpaired Student's t-test was used in Figs. 7 and 8. These tests were performed using the GraphPad Prism software (CA, USA). One symbol $p < .05$, two symbols $p < .01$, three symbols $p < .001$.

Results

Formulation and physical characterization of the liposomes

Liposomes containing tumor antigens (Gp100 and Melan A), the immunostimulatory agent CpG or a fluorescence tracer, calcein, were formulated by the hydration film method using a cationic lipid (DC-cholesterol or DOTAP) and DPPC. The cationic lipid to DPPC molar ratio was 3 to 2. This high proportion of cationic lipid in the liposomes was needed in order to entrap the antigens. The liposomes presented a size below 175 nm with a low polydispersity index (Table 1). The cationic lipids provided a positive Zeta potential to the liposomes and thereby a good dispersibility and stability. Liposome size and zeta potential showed good stability during storage at room temperature over 2 weeks (Fig. S2A-B). DC-cholesterol and DOTAP liposomes encapsulating the tumor antigens and CpG were bigger and carried more positive electric charges than empty and calcein liposomes (Kruskal-Wallis test, $p < 0.05$). Cationic lipids were in much larger quantities in the liposomes than any of the negatively-charged encapsulated compounds and they dominate the zeta potential. Encapsulation of the antigens or CpG caused an increase in Zeta potential rather than a decrease because the encapsulation increased the liposome size: the larger the liposome size, the larger the cationic lipid quantity per liposome, the larger its zeta potential. The encapsulation efficiency of the liposomes varied from 48% to 100%, according to the compound encapsulated and the liposome composition (Table 1). It increased from the antigen Gp100, Melan A, calcein to CpG. The antigens were generally better encapsulated in DOTAP liposomes than they were in DC-cholesterol liposomes (Mann-Whitney test, $p < 0.01$ in case of Melan A). Co-encapsulation of the tumor antigens and CpG did not affect their respective encapsulation efficiency. The leakage of the compounds from the liposomes involved 47%, 0.4% and 14% of the loaded quantity for the Gp100 peptide, CpG and calcein, respectively, just after liposomes formulation (Fig. S2C). Although the leakage was substantial for Gp100, it was not higher for any of the compounds following storage at room temperature for 7 days or 14 days than just after formulation.

Table 1: Physical characterization of the liposomes

	Size (nm)	PDI	Zeta Potential (mV)	EE (%)
DC-cholesterol/DPPC				
Empty liposomes	88 ± 1	0.09 ± 0.01	+36.6 ± 0.9	-
Gp100 Melan A	166.8 ± 0.7	0.24 ± 0.01	+70 ± 2	50 ± 14 67 ± 8
CpG	160 ± 8	0.14 ± 0.02	+52 ± 3	100 ± 0
Gp100 Melan A CpG	172 ± 21	0.21 ± 0.04	+59 ± 10	48 ± 21 69 ± 13 100 ± 0
Calcein	91 ± 2	0.11 ± 0.02	+40 ± 2	93.3 ± 0.4
DOTAP/DPPC				
Empty liposomes	134 ± 18	0.07 ± 0.04	+52 ± 2	-
Gp100 Melan A	152 ± 10	0.15 ±0.07	+56 ± 6	72 ±13 91 ± 3
CpG	169 ± 21	0.12 ± 0.02	+58 ± 11	99.8 ± 0.4
Gp100 Melan A CpG	165 ±17	0.15 ± 0.05	+56 ± 11	71 ±15 82 ± 6 99.6 ± 0.5
Calcein	134 ± 5	0.12 ±0.05	+36 ± 5	90 ± 5

PDI, polydispersity index; EE, encapsulation efficiency.
The data represent the mean values (± SD) of 3 to 9 liposome preparations.

Analysis of liposome morphology by transmission electron microscopy showed that DC-cholesterol and DPPC formed lipid bilayer aggregates and snail-shaped lipid bilayer structures (Fig. 1A). DOTAP liposomes appeared as aggregates of multi-lamellar vesicles. Each multi-lamellar vesicle contained between 10 to 15 bilayers and were 30 nm to 110 nm in size (Fig. 1B).

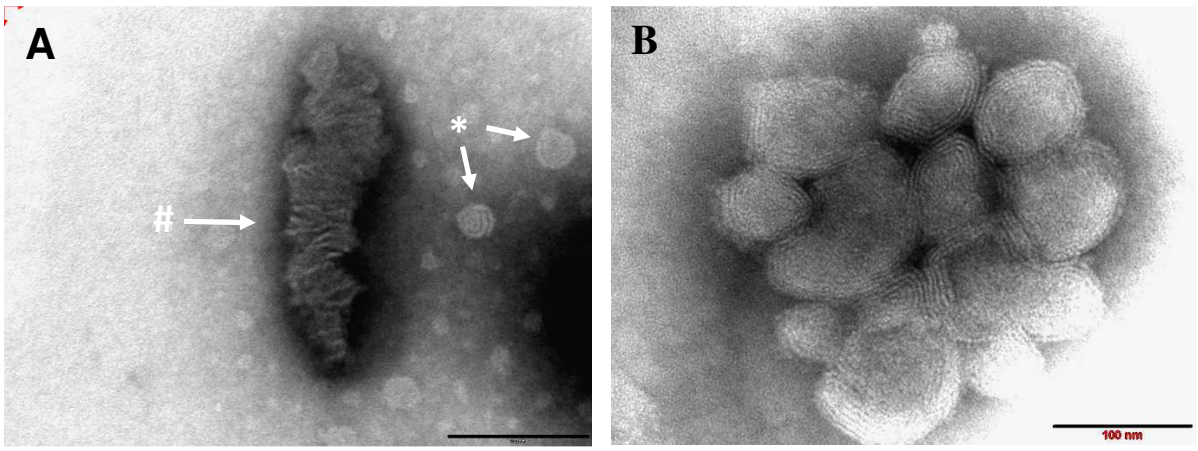

Fig. 1. Morphologies of DC-Cholesterol (A) and DOTAP (B) liposomes visualized by transmission electron microscopy. DC-cholesterol and DPPC formed lipid bilayer aggregates (#) and snail-shaped lipid bilayer structures (*) while DOTAP and DPPC formed aggregates of multi-lamellar vesicles. The scale bars are 100 nm.

The liposomes immediately released a significant fraction of the encapsulated tumor antigens and calcein when placed in saline at 37°C *in vitro*. The remaining fraction remained entrapped within the liposomes and was not released for up to 24 h (Fig. 2). However, the total amount of CpG encapsulated remained entrapped within the liposomes and was not released at all over 24 h (Fig. 2C). DOTAP liposomes better held the antigens than DC-cholesterol liposomes did. DC-cholesterol liposomes were not able to held Gp100 at all since its transport profile across the dialysis membrane was not statistically different from the Gp100 solution (Fig. 2A). Calcein was significantly held by both types of liposomes. However, DC-cholesterol liposomes retained a larger amount of calcein (Fig. 2D).

Therefore, cationic nanoliposomes loaded with vaccine antigens, an adjuvant or a fluorescent tracer were successfully prepared. Although they could not provide the sustained release of the actives *in vitro*, DOTAP liposomes could permanently entrap a large fraction of the actives both in saline at 37°C and during storage at room temperature (Figs. 2 and S2C).

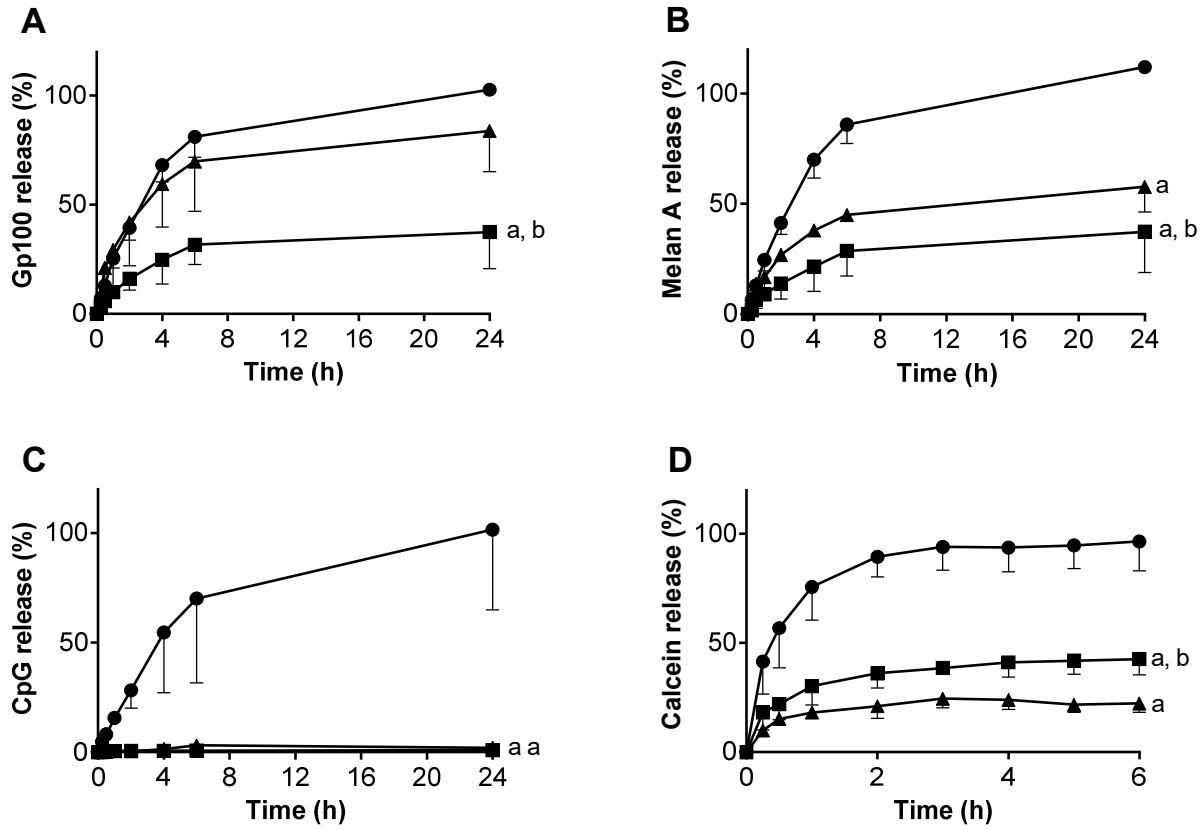

Fig. 2. Release of different compounds from DC-cholesterol and DOTAP liposomes. Liposomes (3 mg of lipids per 0.15 ml of water) were placed in a dialysis bag and compounds were released in 7.5 ml of PBS pH 7.4 at 37°C. A: Gp100; B: Melan A; C: CpG and D: Calcein. Solution (●), DOTAP liposomes (■) and DC-cholesterol liposomes (▲). Two-way ANOVA test with Bonferroni post-test was performed and liposomes were compared to the solution (a, $p<0.05$ vs the solution; b, $p<0.05$ vs DC-cholesterol liposomes). The data represent the mean values (± SD) of 2 to 6 liposome preparations.

Cytotoxicity, cell uptake and cell stimulation in vitro

In vitro cytotoxicity studies indicated that DC-cholesterol liposomes were toxic to Calu-3 cells, a bronchial epithelial cell line, at the lowest lipid concentration explored of 6.25 µg/ml (3.25 µg/ml DC-cholesterol) and to JAWS II cells, a dendritic cell line, from the lipid concentration of 62.5 µg/ml (32.5 µg/ml DC-cholesterol; Fig. 3). However, DOTAP liposomes did not show any cytotoxicity in these cell lines, except at the highest lipid concentration of 500 µg/ml (295 µg/ml DOTAP) in JAWS II cells. Therefore, we selected DOTAP liposomes to pursue the work and gave up DC-cholesterol liposomes because of their cytotoxicity.

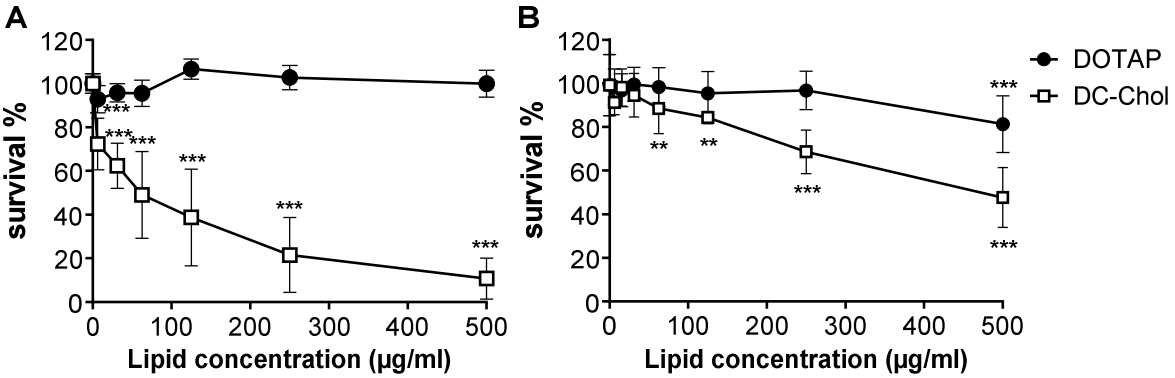

Fig. 3. Cytotoxicity of DOTAP and DC-Cholesterol liposomes evaluated by the MTT assay in Calu-3 (A) or JAWS II (B) cells after 24 h incubation. One-way ANOVA test with Dunnett post-test was performed and the different lipid concentrations were compared to the zero lipid concentration ($p < 0.01$ **; $p < 0.001$ ***). The data represent the mean values (± SD) of 6 to 14 wells.

The efficiency of DOTAP liposomes uptake by DCs and macrophages was assessed *in vitro* using calcein as a tracer of the liposomes and flow cytometry. We chose the MHS alveolar macrophage cell line and the J774 interstitial macrophage cell line for this assay. MHS cells are murine alveolar macrophages immortalized using the SV40 virus and J774 cells are derived from a murine reticulum cell sarcoma. Calcein was taken up in much larger quantities by all cells *in vitro* when encapsulated in liposomes than when in solution, indicating a good phagocytic activity of all cell types (Fig. 4). However, MHS alveolar macrophages and JAWS II dendritic cells took up larger quantities of calcein liposomes than J774 interstitial macrophages did.

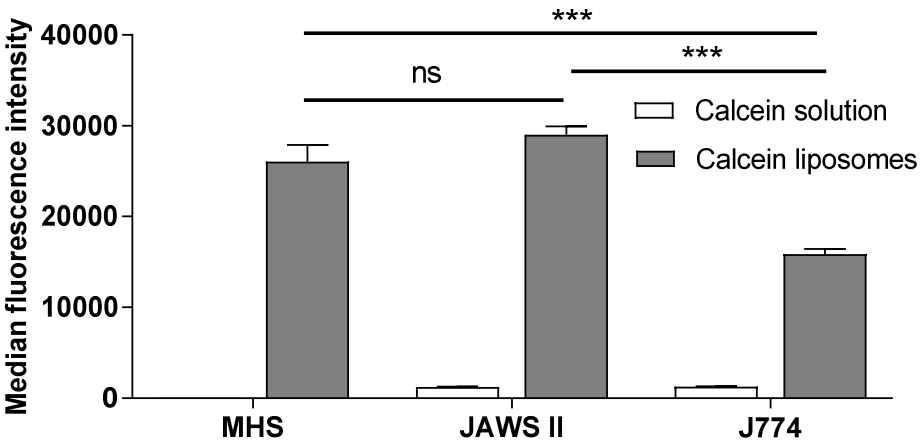

Fig. 4. Uptake of calcein in solution (5 µg calcein/well) or in DOTAP liposomes (5 µg calcein in 370 µg lipids/well) by MHS alveolar macrophages (A), JAWS II dendritic cells (B) and J774 interstitial macrophages after 4 h incubation at 37°C. One-way ANOVA test with Tukey post-test was performed and indicated a higher liposomes uptake by MHS alveolar macrophages and JAWS II dendritic cells than by J774 macrophages ($p < 0.001$). The data represent the mean values (± SD) of 3 assays. Untreated cells showed negligible fluorescence.

The stimulation of alveolar macrophages by DOTAP liposomes and CpG was assessed on MHS alveolar macrophages *in vitro*. Only liposomal CpG induced the secretion of interleukin-6 (IL-6) by MHS cells (Fig. 5). Neither empty DOTAP liposomes nor CpG in solution induced any detectable IL-6 levels, probably because of the low exposure concentrations used.

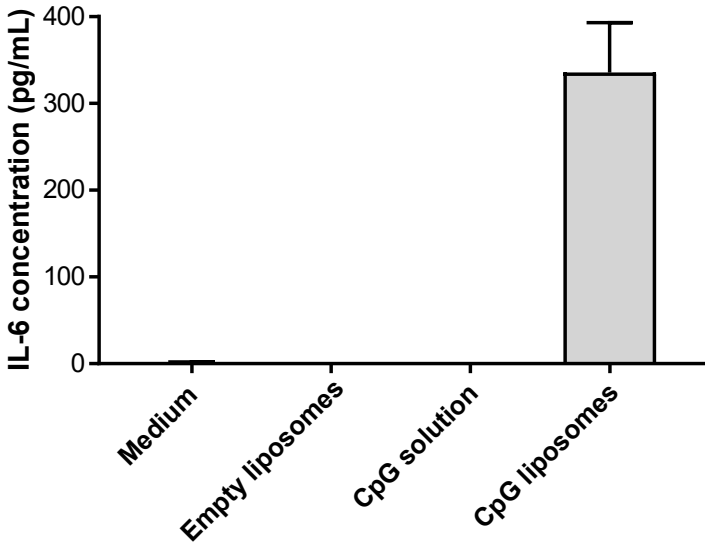

Fig. 5. Stimulation of MHS alveolar macrophages by DOTAP liposomes and CpG. MHS cells were exposed to empty DOTAP liposomes (50 µg lipids/well), CpG in solution (1 µg CpG/well) or in DOTAP liposomes (1 µg CpG/well in 50 µg lipids/well) for 2 hours. Cell supernatants were removed and replaced by fresh medium and the cells were incubated further for 24 h. Cell supernatants were then collected and assayed for IL-6 content. One-way ANOVA test with Dunnett post-test indicated a high

immune stimulation by CpG liposomes ($p < 0.001$ vs medium) and no immune stimulation by CpG in solution and empty liposomes ($p > 0.99$ vs medium). The data represent the mean values (± SD) of 3 to 5 replicates.

Biodistribution in vivo

A biodistribution study of calcein-loaded DOTAP liposomes was carried out in the murine lungs *in vivo* using confocal laser scanning microscopy. It showed that calcein was taken up by phagocytic cells of the pulmonary tissue when delivered in liposomes (Fig. 6). No cell uptake was noticed when calcein was delivered as a solution (Fig. 6B).

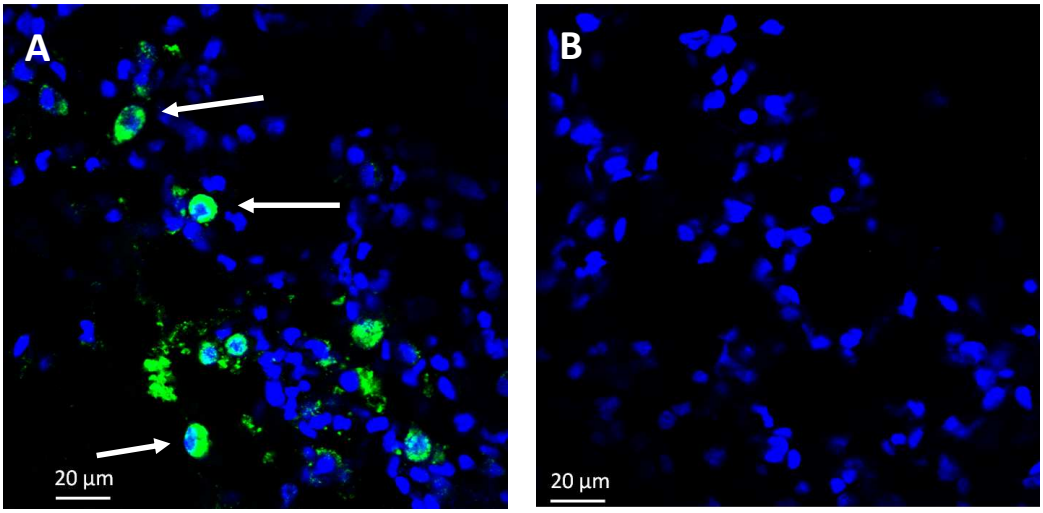

Fig. 6. Localization of calcein in mouse lungs by confocal laser scanning microscopy. The lung tissue was visualized 1 h following delivery of calcein (green) to the lungs. Calcein-loaded DOTAP liposomes (A; 5 µg calcein in 370 µg lipids) or a solution of calcein (B; 5 µg calcein in PBS) was delivered. The lung tissue was colored in blue with nuclear stain DRAQ5™ and the arrows indicate pulmonary cells loading the fluorescent liposomes. The scale bars are 20 µm.

We then assessed whether these phagocytes were AMs, IMs and/or DCs using flow cytometry. Because an intense uptake of calcein liposomes by lung phagocytes was already visible 1 h post-delivery (Fig. 6), we performed the flow cytometry study at this time point as well. Only AMs significantly took up calcein liposomes as their mean fluorescence intensities (MFIs) was 7-times higher than MFIs of AMs exposed to calcein in solution (Fig. 7B). In addition, the % of calcein-positive AMs was large (Fig. 7A). Interstitial macrophages did not take up calcein liposomes more than they took up soluble calcein as the % of calcein-positive IMs and their mean MFIs were similar following *in vivo* exposure to soluble or liposomal calcein. The % of calcein-positive DCs were <1%. However, the % of calcein-positive DCs was 7-times higher when calcein was in liposomes rather than in soluble form. The MFI of calcein-positive DCs are not presented because they comprised too few cells. Following exposure to liposomal calcein, the % of calcein-positive cells were 50% for AMs recovered by BAL. This percentage decreased to 20% for AMs recovered from the lungs, to 10% for IMs

recovered from the lungs and to <1% for DCs recovered from the lungs (Fig. 7). AMs recovered by BAL or AMs recovered from the lungs are the same cells. Therefore, the decrease in % of calcein-positive cells following AMs recovery from the lungs indicates that the procedure of lung digestion and cell labeling probably caused a partial loss of calcein from the cells.

In order to see whether the stimulation of the innate immune system could alter phagocytes uptake of calcein liposomes, we delivered CpG liposomes to the lungs of mice thrice 5 days apart and delivered calcein liposomes or solution one day after the last administration of the CpG liposomes. The stimulation of the innate immune system in the lungs largely enhanced both the % of calcein-positive cells and the significance of calcein uptake (Fig. 8). The % of calcein-positive AMs, IMs and DCs almost doubled following immune stimulation. Ninety percent of AMs from BAL took up liposomal calcein while 55% of them took up soluble calcein. This difference in % of calcein-positive cells following intratracheal instillation of liposomal or soluble calcein was also apparent for AMs from the lungs, IMs and DCs (Fig. 8). However, it was only significant for AMs from BAL. In addition, the MFI ratios of AMs exposed to calcein liposomes vs calcein solution largely increased following immune stimulation. These ratios were respectively 7 and 28 without and with immune stimulation for AMs collected by BAL and 2.5 and 3.3 for AMs isolated from the lungs (Figs. 7 and 8). The ratio was worth 2.2 in case of DCs in stimulated lungs. By contrast, the MFI of IMs exposed to calcein solution or liposomes remained equivalent following immune stimulation, as they were without immune stimulation. An example of AM populations collected by BAL and from the lungs in the cases of immune stimulation and no stimulation is presented in Fig. 9. The AM populations are presented in terms of their fluorescence intensity in the calcein channel. The figures well demonstrate the large uptake of calcein liposomes as well as the large enhancement in uptake following immune stimulation using liposomal CpG.

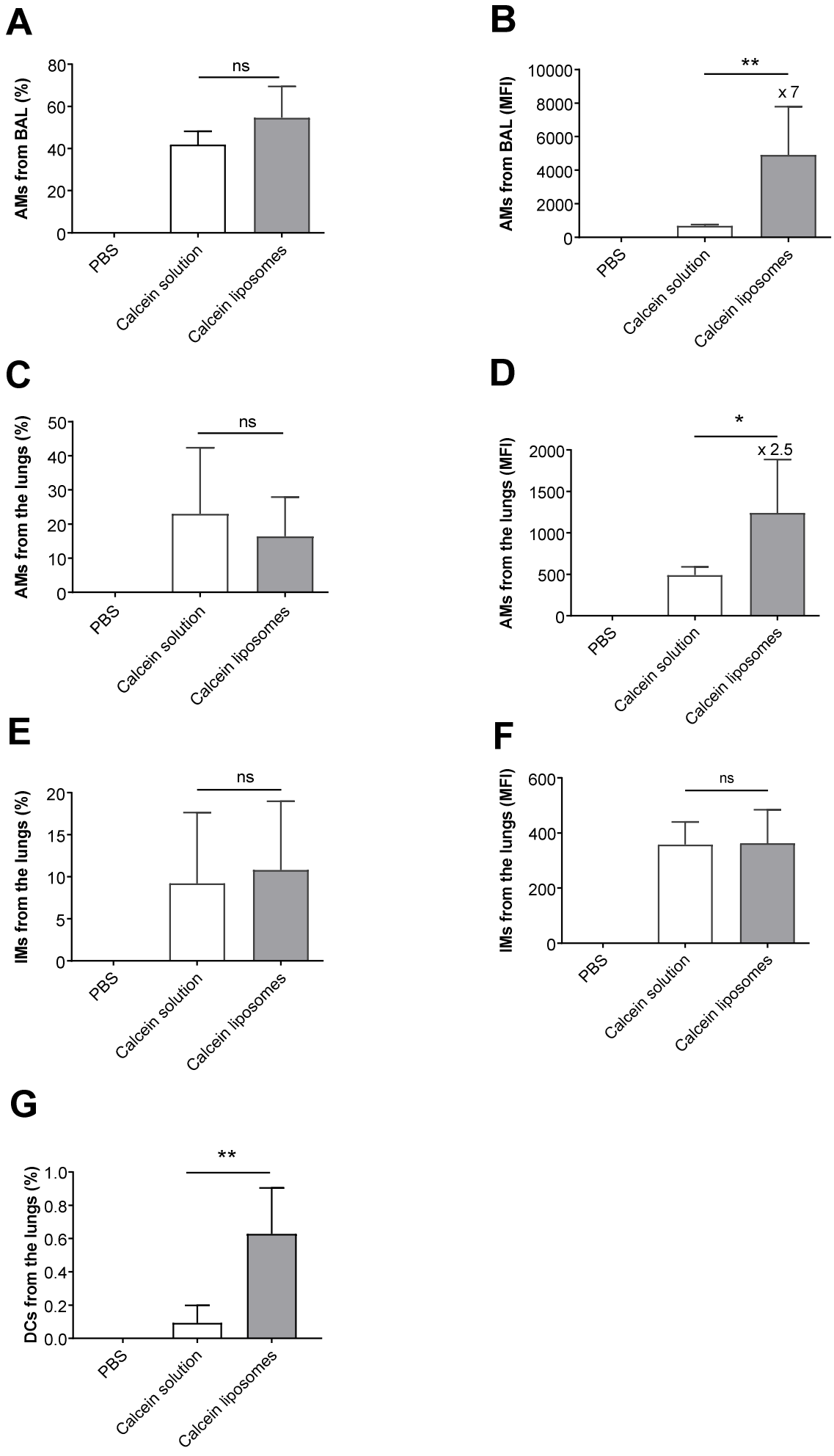
A
AMs from BAL (%)
80
60
40
20
0
ns
PBS
Calcein solution
Calcein liposomes
B
AMs from BAL (MFI)
10000
8000
6000
4000
2000
0
**
x 7
PBS
Calcein solution
Calcein liposomes
C
AMs from the lungs (%)
50
40
30
20
10
0
ns
PBS
Calcein solution
Calcein liposomes
D
AMs from the lungs (MFI)
2000
1500
1000
500
0
*
x 2.5
PBS
Calcein solution
Calcein liposomes
E
IMs from the lungs (%)
20
15
10
5
0
ns
PBS
Calcein solution
Calcein liposomes
F
IMs from the lungs (MFI)
600
400
200
0
ns
PBS
Calcein solution
Calcein liposomes
G
DCs from the lungs (%)
1.0
0.8
0.6
0.4
0.2
0.0
**
PBS
Calcein solution
Calcein liposomes

Fig. 7. Fraction and mean fluorescence intensity of calcein-positive alveolar macrophages (AMs), interstitial macrophages (IMs) and dendritic cells (DCs) 1 h following delivery of 5 µg calcein in DOTAP liposomes (370 µg lipids) or solution to the lungs of healthy mice. Alveolar macrophages were collected by bronchoalveolar lavage (BAL) or after lung resection and digestion. Interstitial macrophages and DC were only analysed in the lungs after resection and digestion. The data represent the mean values (± SD) of 4 to 5 mice.
.

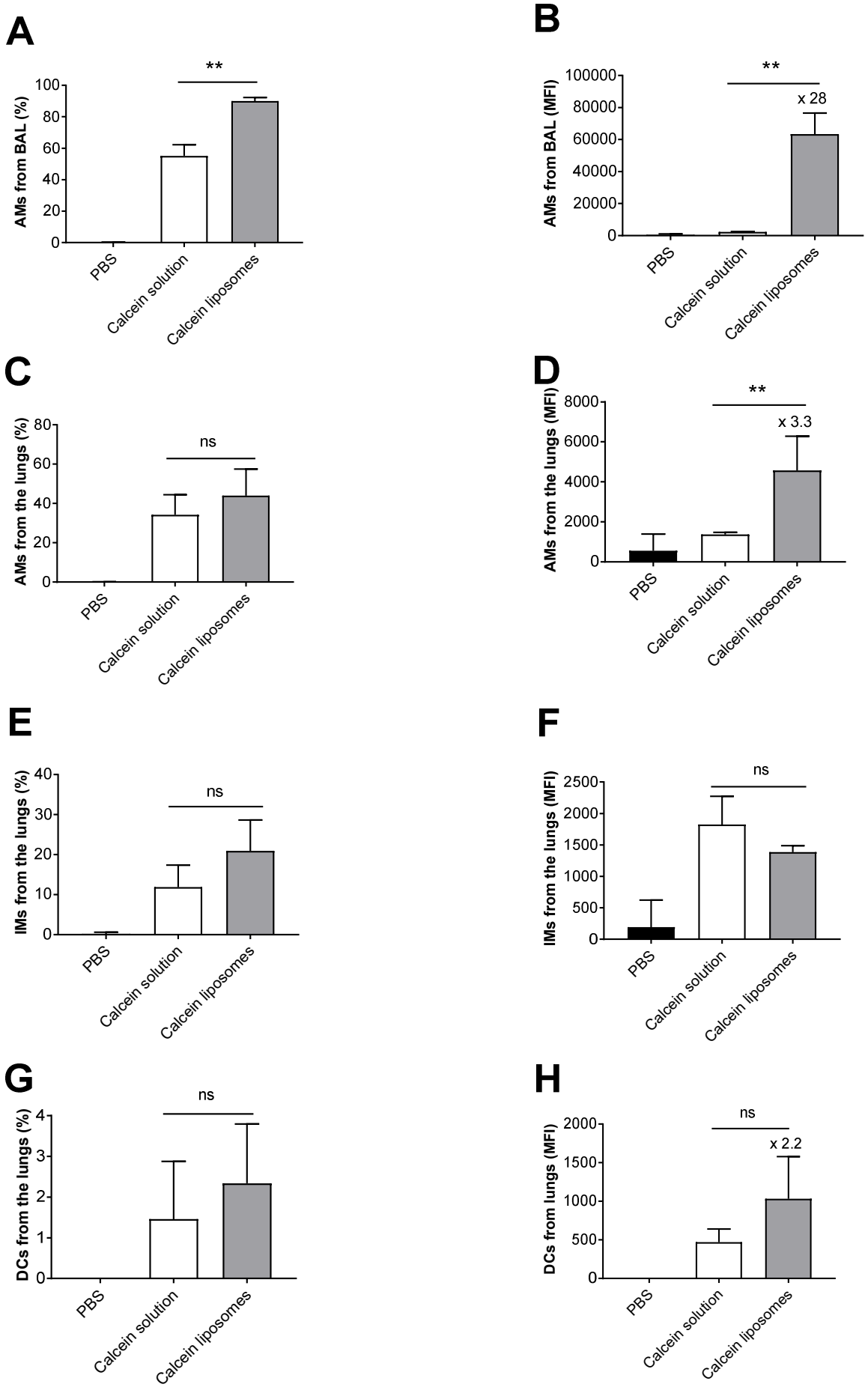
A
AMs from BAL (%)
100
80
60
40
20
0
**
PBS
Calcein solution
Calcein liposomes
B
AMs from BAL (MFI)
100000
80000
60000
40000
20000
0
**
x 28
PBS
Calcein solution
Calcein liposomes
C
AMs from the lungs (%)
80
60
40
20
0
ns
PBS
Calcein solution
Calcein liposomes
D
AMs from the lungs (MFI)
8000
6000
4000
2000
0
**
x 3.3
PBS
Calcein solution
Calcein liposomes
E
IMs from the lungs (%)
40
30
20
10
0
ns
PBS
Calcein solution
Calcein liposomes
F
IMs from the lungs (MFI)
2500
2000
1500
1000
500
0
ns
PBS
Calcein solution
Calcein liposomes
G
DCs from the lungs (%)
4
3
2
1
0
ns
PBS
Calcein solution
Calcein liposomes
H
DCs from lungs (MFI)
2000
1500
1000
500
0
ns
x 2.2
PBS
Calcein solution
Calcein liposomes

Fig. 8. Fraction and mean fluorescence intensity of calcein-positive alveolar macrophages (AMs), interstitial macrophages (IMs) and dendritic cells (DCs) 1 h following delivery of 5 µg calcein in DOTAP liposomes (370 µg lipids) or solution to the lungs of immune-stimulated mice. The innate immune system in the lungs was stimulated by intratracheal instillation of liposome-encapsulated CpG (1 µg of CpG in 50 µg lipids) thrice 5 days apart. Calcein liposomes or solution was then delivered by intratracheal instillation one day after the last administration of CpG liposomes. Alveolar macrophages were collected by bronchoalveolar lavage (BAL) or after lung resection and digestion. Interstitial macrophages and DCs were only analysed in the lungs after resection and digestion. The data represent the mean values (± SD) of 5 mice.

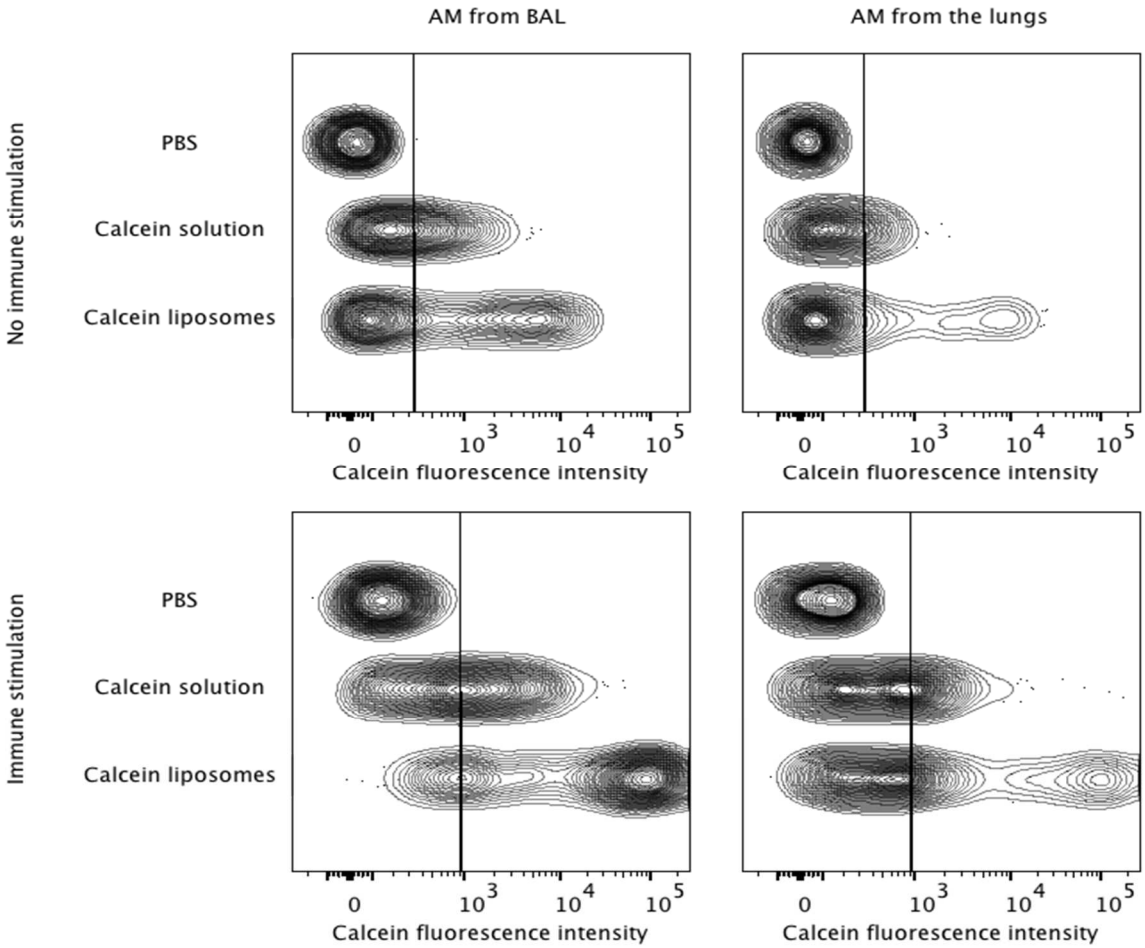

Fig. 9. Representative populations of alveolar macrophages collected by bronchoalveolar lavage or by using lung digestion in terms of calcein fluorescence in conditions of non-immune stimulation and immune stimulation using CpG liposomes.

Discussion

This study showed that DC-cholesterol and DOTAP liposomes could permanently entrap peptide antigens, vaccine adjuvants and fluorescent dyes but that they could not sustain their release *in vitro*. DOTAP liposomes were safe to respiratory cells but DC-cholesterol liposomes showed cytotoxicity in the two cell lines tested. Encapsulation of the fluorescent dye calcein in DOTAP liposomes strongly promoted its uptake by macrophages and DCs *in vitro*. However, uptake of liposomal calcein was observed in a large fraction of AMs but in very few DCs *in vivo*. Stimulation of the innate immune system by liposomal CpG triggered alveolar macrophages to secrete IL-6 *in vitro* and largely enhanced calcein uptake by all phagocytes in the lungs *in vivo*.

AMs constituted the main cell type involved in the uptake of nanoliposomes in the lungs *in vivo*. Few DCs took up the cationic liposomes and IMs did not take up liposomal calcein more than they took up soluble calcein. These results are in line with previous investigations. Blank et al. delivered polystyrene particles by intranasal instillation to the lungs of mice[9]. Their particles ranged from 20 nm to 1,000 nm in size. The majority of the particles were taken up by AMs, irrespective of size. However, DCs also took up the particles and the 20 nm and 50 nm particles the most. Moreover, particle uptake increased over time and larger uptake was observed 24 h post-delivery than 2 h post-delivery. The calcein liposomes prepared with DOTAP and DPPC in our study were 134 nm in size and therefore larger than the 20 and 50 nm particles of the Blank‘s study. Moreover, we assessed uptake 1 h post-delivery. This time point was selected because it already resulted in an intense liposome uptake by lung phagocytes in the confocal imaging studies. This uptake was then confirmed by the flow cytometry studies as 50% and 90% of AMs took up calcein liposomes in the unstimulated and stimulated lungs, respectively, 1 h post-delivery. Yet, an assessment at a later time point might have resulted in the observation of larger DCs uptake. In a triple cell co-culture model composed of a monolayer of lung epithelial cells, macrophages added on top of the epithelium and DCs underneath, particle clearance mainly resulted from the highly phagocytic nature of macrophages as well[19]. However, macrophages also appeared to transfer particulate antigen to DCs via cell-cell contacts over time. Fromen et al. delivered cationic or anionic 80 x 80 x 320 nm rod-shaped particles to the lungs of mice and measured phagocyte particle uptake and lung tissue stimulation 72 h post-intratracheal instillation[10]. Again, AMs readily internalized both particle types. However, a larger number of DCs took up cationic nanoparticles than anionic nanoparticles. Finally, Blom et al. delivered 100 nm liposomes or 100 nm virosomes to the lungs of mice and measured macrophage and DC uptake in the lung tissue 24 h after delivery[20]. Macrophages, and to a lesser extent DCs, captured particles, with no difference in uptake between virosomes and liposomes.

However, our study went steps further compared with these previous ones. In fact, we highlighted the benefit of the encapsulation in liposomes by measuring both the uptake of soluble and liposomal calcein and we assessed the uptake by IMs, in addition to AMs and DCs. The encapsulation increased the targeting of both AMs and DCs, but not of IMs. Although J774 macrophages, representative of IMs, were twice less phagocytic than MHS AMs and JAWS II DCs *in vitro*, all the cells were highly phagocytic and differences in phagocytic activity might not explain our *in vivo* data. Rather, the localization of the phagocytes in the lungs and their

accessibility to the liposomes are a more probable explanation for the differences in liposomes uptake[5]. Alveolar macrophages were the lung phagocytes the most exposed to the liposomes since they are located in the airway lumen and alveolar space where the liposomes deposited after intratracheal instillation. At the opposite, IMs had the least accessibility to the liposomes since IMs are located in the lung interstitium beneath the respiratory epithelium. Dendritic cells presented an intermediate accessibility to the liposomes because they are located in the lung parenchyma with dendrites extending in the airway lumen.

Calcein uptake by phagocytes was also measured after stimulation of the innate immune system in the lungs by liposomal CpG. Studying the fate of nanocarriers in the stimulated lungs is relevant because pulmonary vaccination will most frequently involve booster doses[21]. Unmethylated cytosine-phosphate-guanine motifs are pathogen-associated molecular patterns as they are prevalent in bacterial but not vertebrate genomic DNA[22]. These motifs are recognized by the pattern recognition receptor toll-like receptor 9 (TLR9) and activate natural killer cells, macrophages, B cells and DCs. CpG is currently included in the composition of one injectable vaccine approved for the prevention of hepatitis B virus infection in adults and it is investigated as immunostimulant for the immunotherapy of lung cancer[23, 24]. The particular CpG molecule used in the present study has previously been shown to transiently increase AM numbers in the lungs of healthy mice without causing an influx of inflammatory cells[25]. Here, immune stimulation with liposomal CpG largely increased calcein uptake by all phagocytes in the lungs. It increased the number of calcein-positive AMs, IMs and DCs but it also significantly increased the efficiency of the nanoliposomes targeting to AMs and DCs. In view of the large AM uptake of liposomal calcein, liposomal CpG probably ended up in AMs as well. The TLR9 recognized by CpG is located within the endosome and liposomes thus delivered CpG directly to its receptor. The high efficacy of the liposomes to address CpG to its receptor is demonstrated by the tremendous IL-6 production by AMs in culture following exposure to liposomal CpG. Fernandez et al showed that CpG stimulation of TLR9 in AMs allowed AMs to overcome IL-10-mediated inhibition and to behave in a proinflammatory manner[26]. It remains to be determined whether the increased uptake of calcein lipoomes by all phagocytes resulted from a direct CpG stimulation on individual cell types or an indirect stimulation through AM activation.

Liposomes made of DC-cholesterol and DPPC or made of DOTAP and DPPC could permanently entrap actives but could not release them over time. The ability of liposomes to gradually release actives strongly depends on the rigidity of the bilayer membrane of the liposomes. The liposome membrane will only be rigid if its transition temperature from the gel to the liquid phase is above the body temperature. Barnier Quer et al. measured a phase transition temperature of 38°C for DC-cholesterol/DPPC liposomes where DC-cholesterol was present at 10 mole %. However, above 30 mole % DC-cholesterol (and our formulation contained 60 mole % DC-cholesterol), a liquid-ordered phase was induced and no phase transition temperature could be measured[27]. Cinelli et al. measured the thermal behavior of pure DPPC and mixed DOTAP/DPPC bilayer membranes. The transition temperature of pure DPPC was 41°C and it progressively shifted to lower temperatures to reach approximately 20°C at 60 mole % DOTAP, the mole % DOTAP in our DOTAP liposomes[28]. Therefore, the absence of sustained release of the actives from our liposomes is consistent with their low phase transition temperature. However, our liposomes were able to retain peptide antigens, CpG and calcein at

610 room temperature for at least two weeks. Because these compounds all carried negative charges,
611 they probably bound to the cationic lipids in the liposomes by strong electrostatic interactions[29].
612 Both the melan A and Gp100 antigens carry one negative charge. CpG carries 20 negative
613 charges and calcein carries 4 negative charges. The high number of charges per CpG molecule
614 is probably the reason why CpG encapsulation efficiency was close to 100% as well as the
615 reason why the total amount of CpG encapsulated remained entrapped within the liposomes
616 and was not released at all. Similarly, the high negative charge of the calcein molecule could
617 explain its high encapsulation efficiency in our cationic liposomes[30].
618 Liposomes made of DOTAP and DPPC formed aggregated multi-lamellar vesicles. The
619 size of the individual multi-lamellar vesicles within the aggregates ranged between 30 nm and
620 110 nm and the size of vesicle aggregates ranged between 130 nm and 170 nm. DC-cholesterol
621 and DPPC formed 30 nm snail-shaped lipid bilayer structures and aggregates of lipid bilayers
622 with sizes varying from 90 nm to 175 nm. However, they did not form closed vesicles. The
623 absence of closed vesicles in the DC-cholesterol/DPPC preparation is also consistent with the
624 lack of sustained release of the actives. Although liposomes of similar composition have already
625 been prepared, these studies did not examine liposome morphologies using microscopy
626 techniques[13, 27, 31]. However, morphologies can unravel encapsulation and release properties of
627 the liposomes.
628 The liposomes made of DC-cholesterol induced cytotoxicity in Calu-3 cells, a bronchial
629 epithelial cell line, at the lowest lipid concentration explored of 6.25 μg/ml (3.25 μg/ml of DC-
630 cholesterol) as well as in JAWS II dendritic cells at the lipid concentration of 62.5 μg/ml (32.5
631 μg/ml of DC-cholesterol). However, DOTAP liposomes were safe in these cell lines up to a
632 lipid concentration of 250 μg/ml (147.5 μg/ml of DOTAP). The potential toxicity of cationic
633 lipids is well known[32]. Toxicity depends among others on the nature of the cationic lipid, the
634 nature of the co-lipid, the proportion of the different lipids and the cell type. Lechanteur et al
635 similarly showed higher toxicity of DC-cholesterol over DOTAP in A549 cells, a type II
636 alveolar epithelial cell line[13]. At a 1:1 molar ratio with the fusogenic
637 dioleoylphosphatidylethanolamine (DOPE) phospholipid, DC-cholesterol was safe up to a
638 concentration of 2.7 μg/ml in the A549 cell line while DOTAP was safe up to a concentration
639 of 7 μg/ml. Filion and Phillips observed cytotoxicity of cationic lipids alone, including DOTAP
640 at a concentration of 70 μg/ml, in murine macrophages and the human monocyte U937 cell line.
641 However, toxicity of the cationic lipids was enhanced by the presence of DOPE. The
642 replacement of DOPE by DPPC significantly reduced liposome cytotoxicity and the presence
643 of dipalmitoylphosphatidylethanolamine-PEG in the liposomes completely abolished it[31].
644 Therefore, these previous cytotoxicity data corrobate our own observations.
645
646
647 **Conclusion**
648
649 Nanoliposomes made of a cationic lipid and DPPC could permanently entrap peptide
650 antigens, CpG and the fluorescent dye calcein. However, they could not sustain the release of
651 these compounds *in vitro*, presumably as a result of the low phase transition temperature of the
652 lipid bilayers. DOTAP liposomes were safe to respiratory cells *in vitro* while those composed
653 of DC-cholesterol were cytotoxic. Calcein encapsulation in nanoliposomes slightly improved

the targeting of the fluorescent dye to DCs in the lungs *in vivo*. However, the access to DCs was largely hindered by AMs since the majority of the nanoliposomes were taken up by these cells in the airway and alveolar lumen. Targeting of IMs could not be achieved by using the nanoliposomes, probably due to IMs localization in the lung parenchyma beneath the airway epithelium. Stimulation of the innate immune system strongly enhanced calcein uptake by all phagocytes in the lungs. It increased the number of calcein-positive AMs, IMs and DCs but it also significantly increased the efficiency of nanoliposomes uptake by AMs. Future studies will aim to assess the protection conferred by these formulations to lung tumor growth in murine models of lung cancer.

Acknowledgments

This work was supported by a research grant (grant number: 3.4503.12) of the Fonds National de la Recherche Scientifique (FNRS, Belgium). Rita Vanbever, François Huaux and Donatienne Tyteca are Research Director, Senior Research Associate and Research Associate of the FNRS, respectively.

Supporting information. Gating strategies of the flow cytometry studies (Fig. S1); colloidal stability of nanoliposomes (Fig. S2).

References:

1. Organization, W. H. Fact sheet, Cancer. **2017**.
2. Forde, P. M.; Kelly, R. J.; Brahmer, J. R. New strategies in lung cancer: translating immunotherapy into clinical practice. *Clin Cancer Res* **2014,** *20*, (5), 1067-73.
3. Ott, P. A.; Hu, Z.; Keskin, D. B.; Shukla, S. A.; Sun, J.; Bozym, D. J.; Zhang, W.; Luoma, A.; Giobbie-Hurder, A.; Peter, L.; Chen, C.; Olive, O.; Carter, T. A.; Li, S.; Lieb, D. J.; Eisenhaure, T.; Gjini, E.; Stevens, J.; Lane, W. J.; Javeri, I.; Nellaiappan, K.; Salazar, A. M.; Daley, H.; Seaman, M.; Buchbinder, E. I.; Yoon, C. H.; Harden, M.; Lennon, N.; Gabriel, S.; Rodig, S. J.; Barouch, D. H.; Aster, J. C.; Getz, G.; Wucherpfennig, K.; Neuberg, D.; Ritz, J.; Lander, E. S.; Fritsch, E. F.; Hacohen, N.; Wu, C. J. An immunogenic personal neoantigen vaccine for patients with melanoma. *Nature* **2017,** *547*, (7662), 217-221.
4. Tonnis, W. F.; Kersten, G. F.; Frijlink, H. W.; Hinrichs, W. L.; de Boer, A. H.; Amorij, J. P. Pulmonary vaccine delivery: a realistic approach? *J Aerosol Med Pulm Drug Deliv* **2012,** *25*, (5), 249-60.
5. Hoffmann, F.; Ender, F.; Schmudde, I.; Lewkowich, I. P.; Kohl, J.; Konig, P.; Laumonnier, Y. Origin, Localization, and Immunoregulatory Properties of Pulmonary Phagocytes in Allergic Asthma. *Front Immunol* **2016,** *7*, 107.
6. Hussell, T.; Bell, T. J. Alveolar macrophages: plasticity in a tissue-specific context. *Nat Rev Immunol* **2014,** *14*, (2), 81-93.
7. Smith, D. M.; Simon, J. K.; Baker, J. R., Jr. Applications of nanotechnology for immunology. *Nat Rev Immunol* **2013,** *13*, (8), 592-605.
8. Semmler-Behnke, M.; Takenaka, S.; Fertsch, S.; Wenk, A.; Seitz, J.; Mayer, P.; Oberdorster, G.; Kreyling, W. G. Efficient elimination of inhaled nanoparticles from the alveolar region: evidence for

700 interstitial uptake and subsequent reentrainment onto airways epithelium. *Environ Health Perspect*
701 **2007,** *115*, (5), 728-33.
702 9. Blank, F.; Stumbles, P. A.; Seydoux, E.; Holt, P. G.; Fink, A.; Rothen-Rutishauser, B.; Strickland,
703 D. H.; von Garnier, C. Size-dependent uptake of particles by pulmonary antigen-presenting cell
704 populations and trafficking to regional lymph nodes. *Am J Respir Cell Mol Biol* **2013,** *49*, (1), 67-77.
705 10. Fromen, C. A.; Rahhal, T. B.; Robbins, G. R.; Kai, M. P.; Shen, T. W.; Luft, J. C.; DeSimone, J. M.
706 Nanoparticle surface charge impacts distribution, uptake and lymph node trafficking by pulmonary
707 antigen-presenting cells. *Nanomedicine* **2016,** *12*, (3), 677-687.
708 11. Loira-Pastoriza, C.; Todoroff, J.; Vanbever, R. Delivery strategies for sustained drug release in
709 the lungs. *Adv Drug Deliv Rev* **2014,** *75*, 81-91.
710 12. Christensen, D.; Korsholm, K. S.; Rosenkrands, I.; Lindenstrom, T.; Andersen, P.; Agger, E. M.
711 Cationic liposomes as vaccine adjuvants. *Expert Rev Vaccines* **2007,** *6*, (5), 785-96.
712 13. Lechanteur, A.; Sanna, V.; Duchemin, A.; Evrard, B.; Mottet, D.; Piel, G. Cationic Liposomes
713 Carrying siRNA: Impact of Lipid Composition on Physicochemical Properties, Cytotoxicity and
714 Endosomal Escape. *Nanomaterials (Basel)* **2018,** *8*, (5).
715 14. Lombry, C.; Bosquillon, C.; Preat, V.; Vanbever, R. Confocal imaging of rat lungs following
716 intratracheal delivery of dry powders or solutions of fluorescent probes. *J Control Release* **2002,** *83*,
717 (3), 331-41.
718 15. Koussoroplis, S. J.; Paulissen, G.; Tyteca, D.; Goldansaz, H.; Todoroff, J.; Barilly, C.; Uyttenhove,
719 C.; Van Snick, J.; Cataldo, D.; Vanbever, R. PEGylation of antibody fragments greatly increases their
720 local residence time following delivery to the respiratory tract. *J Control Release* **2014,** *187*, 91-100.
721 16. Guilliams, M.; De Kleer, I.; Henri, S.; Post, S.; Vanhoutte, L.; De Prijck, S.; Deswarte, K.; Malissen,
722 B.; Hammad, H.; Lambrecht, B. N. Alveolar macrophages develop from fetal monocytes that
723 differentiate into long-lived cells in the first week of life via GM-CSF. *J Exp Med* **2013,** *210*, (10), 1977-
724 92.
725 17. Bedoret, D.; Wallemacq, H.; Marichal, T.; Desmet, C.; Quesada Calvo, F.; Henry, E.; Closset, R.;
726 Dewals, B.; Thielen, C.; Gustin, P.; de Leval, L.; Van Rooijen, N.; Le Moine, A.; Vanderplasschen, A.;
727 Cataldo, D.; Drion, P. V.; Moser, M.; Lekeux, P.; Bureau, F. Lung interstitial macrophages alter dendritic
728 cell functions to prevent airway allergy in mice. *J Clin Invest* **2009,** *119*, (12), 3723-38.
729 18. Becher, B.; Schlitzer, A.; Chen, J.; Mair, F.; Sumatoh, H. R.; Teng, K. W.; Low, D.; Ruedl, C.;
730 Riccardi-Castagnoli, P.; Poidinger, M.; Greter, M.; Ginhoux, F.; Newell, E. W. High-dimensional analysis
731 of the murine myeloid cell system. *Nat Immunol* **2014,** *15*, (12), 1181-9.
732 19. Blank, F.; Rothen-Rutishauser, B.; Gehr, P. Dendritic cells and macrophages form a
733 transepithelial network against foreign particulate antigens. *Am J Respir Cell Mol Biol* **2007,** *36*, (6),
734 669-77.
735 20. Blom, R. A. M.; Amacker, M.; van Dijk, R. M.; Moser, C.; Stumbles, P. A.; Blank, F.; von Garnier,
736 C. Pulmonary Delivery of Virosome-Bound Antigen Enhances Antigen-Specific CD4(+) T Cell
737 Proliferation Compared to Liposome-Bound or Soluble Antigen. *Front Immunol* **2017,** *8*, 359.
738 21. Patil, H. P.; Murugappan, S.; ter Veer, W.; Meijerhof, T.; de Haan, A.; Frijlink, H. W.; Wilschut,
739 J.; Hinrichs, W. L.; Huckriede, A. Evaluation of monophosphoryl lipid A as adjuvant for pulmonary
740 delivered influenza vaccine. *J Control Release* **2014,** *174*, 51-62.
741 22. Krieg, A. M. CpG motifs in bacterial DNA and their immune effects. *Annu Rev Immunol* **2002,**
742 *20*, 709-60.
743 23. Splawn, L. M.; Bailey, C. A.; Medina, J. P.; Cho, J. C. Heplisav-B vaccination for the prevention
744 of hepatitis B virus infection in adults in the United States. *Drugs Today (Barc)* **2018,** *54*, (7), 399-405.
745 24. Gallotta, M.; Assi, H.; Degagne, E.; Kannan, S. K.; Coffman, R. L.; Guiducci, C. Inhaled TLR9
746 Agonist Renders Lung Tumors Permissive to PD-1 Blockade by Promoting Optimal CD4(+) and CD8(+)
747 T-cell Interplay. *Cancer Res* **2018,** *78*, (17), 4943-4956.
748 25. Todoroff, J.; Lemaire, M. M.; Fillee, C.; Jurion, F.; Renauld, J. C.; Huygen, K.; Vanbever, R.
749 Mucosal and systemic immune responses to Mycobacterium tuberculosis antigen 85A following its co-
750 delivery with CpG, MPLA or LTB to the lungs in mice. *PLoS One* **2013,** *8*, (5), e63344.

751 26. Fernandez, S.; Jose, P.; Avdiushko, M. G.; Kaplan, A. M.; Cohen, D. A. Inhibition of IL-10
752 receptor function in alveolar macrophages by Toll-like receptor agonists. *J Immunol* **2004,** *172*, (4),
753 2613-20.
754 27. Barnier Quer, C.; Elsharkawy, A.; Romeijn, S.; Kros, A.; Jiskoot, W. Cationic liposomes as
755 adjuvants for influenza hemagglutinin: more than charge alone. *Eur J Pharm Biopharm* **2012,** *81*, (2),
756 294-302.
757 28. Cinelli, S.; Onori, G.; Zuzzi, S.; Bordi, F.; Cametti, C.; Sennato, S.; Diociaiuti, M. Properties of
758 mixed DOTAP-DPPC bilayer membranes as reported by differential scanning calorimetry and dynamic
759 light scattering measurements. *J Phys Chem B* **2007,** *111*, (33), 10032-9.
760 29. Even-Chen, S.; Cohen, R.; Barenholz, Y. Factors affecting DNA binding and stability of
761 association to cationic liposomes. *Chem Phys Lipids* **2012,** *165*, (4), 414-23.
762 30. Wang, H.; Zhao, P.; Liang, X.; Song, T.; Gong, X.; Niu, R.; Chang, J. Construction of a novel
763 cationic polymeric liposomes formed from PEGlated octadecyl-quaternized lysine modified
764 chitosan/cholesterol for enhancing storage stability and cellular uptake efficiency. *Biotechnol Bioeng*
765 **2010,** *106*, (6), 952-62.
766 31. Filion, M. C.; Phillips, N. C. Toxicity and immunomodulatory activity of liposomal vectors
767 formulated with cationic lipids toward immune effector cells. *Biochim Biophys Acta* **1997,** *1329*, (2),
768 345-56.
769 32. Allen, T. M.; Cullis, P. R. Liposomal drug delivery systems: from concept to clinical applications.
770 *Adv Drug Deliv Rev* **2013,** *65*, (1), 36-48.

771